Electronic structure and optical properties of conjugated molecules: SAC-CI study

Masahiro Ehara, Biswajit Saha, Potjaman Poolmee, Malinee Promkatkaew, Supa Hannongbua et al.

Citation: AIP Conf. Proc. **1504**, 279 (2012); doi: 10.1063/1.4771722
View online: http://dx.doi.org/10.1063/1.4771722
View Table of Contents: http://proceedings.aip.org/dbt/dbt.jsp?KEY=APCPCS&Volume=1504&Issue=1
Published by the American Institute of Physics.

Electronic Structure and Optical Properties of Conjugated Molecules: SAC-CI Study

Masahiro Ehara[†§], Biswajit Saha[$], Potjaman Poolmee[‡], Malinee Promkatkaew[‡], Supa Hannongbua[‡], Yun-peng Lu[¶], and Hiroshi Nakatsuji[#§]

[†]*Institute for Molecular Science, 38 Myodaiji, Okazaki, 444-8585, Japan*
[§]*JST-CREST, Sanboncho-5, Chiyoda-ku, Tokyo 102-0075, Japan*
[$]*Fukui Institute for Fundamental Chemistry, Kyoto University, Sakyo-ku, Kyoto 606-8103, Japan*
[‡]*Department of Chemistry, Faculty of Science, Kasetsart University, Bangkok 10900, Thailand*
[¶]*Division of Chemistry and Biochemistry, School of Physical and Mathematical Sciences, Nanyang Technological University, 21 Nanyang Link, 637371, Singapore*
[#]*Quantum Chemistry Research Institute, Goryo Oohara 1-36, Nishikyo-ku, Kyoto 615-8245, Japan*

Abstract. Electronic structure and optical properties of some organic conjugated molecules, that is the oligomers for organic-light emitting diodes (OLED), chelating hetero-atomic conjugated ligands, and UVB blocking molecules, have been investigated by the SAC-CI method. The absorption and emission spectra of these molecules were reproduced accurately. For OLED molecules, chain length dependence of the excitation and emission energies was evaluated for poly *para*-phenylene vinylene and poly *para*-phenylene. Thermal effect on the electronic spectra of fluorene-thiophene and its derivatives was examined with taking accounts the Boltzmann distribution. The photophysical properties of the chelating hetero-atomic molecules including pyridine-, benxazole-, and benzothiazole derivatives which are useful for electroluminescent metal complex were systematically calculated. The UVB blocking function of the methoxy substituted cinnamates was investigated with regard to the substitution position. The excited-state geometry relaxation of these molecules was interpreted based on the electrostatic force theory. The present work provides a useful basis for the theoretical design predicting the optical properties of the photo-functional molecules.

Keywords: SAC-CI, optical properties, organic-light-emitting diodes, chelating hetero-atomic conjugated ligands, UVB blocking molecules
PACS: 31.15.ag, 31.15.bw, 31.15vq

INTRODUCTION

Photochemistry involving ππ* excited states has shown a rich variety of phenomena that are interesting but cannot be understood without the knowledge of their electronic structure. Recently, these photo-electronic processes and photo-physical properties have been rigorously utilized in the field of technology and industry. The detailed information of the molecular excited states is relevant for developing the photo-functional molecules. On the other hand, development of the accurate state-of-the-art theoretical methodologies has made us possible to obtain the precise knowledge of the excited and ionized states of molecules. Theory can predict the fine details of the excitation and ionization processes and even support for designing new materials. Thus, the interplay between theory and experiment has become relevant in the modern excited-state chemistry.

One of the abovementioned photochemistry, the photo-physical properties of fluorescent molecules like organic light-emitting diodes (OLED) is an attractive and important subject. The OLED is generally recognized as one of the promising candidates for the next generation electro-optical devices. There are two categories in OLED molecules, one is the phosphorescent materials based on the heavy metal complex like Ir(III) complexes which achieve high quantum yield for electroluminescence using triplet states. The other is the polymer materials based on the organic π-conjugated molecules which has advantage for being processed under mild condition, for examples, poly *para*-phenylene vinylene [1-4], poly *para*-phenylene, and fluorene-thiophene [5-7].

International Conference of Computational Methods in Sciences and Engineering 2009
AIP Conf. Proc. 1504, 279-290 (2012); doi: 10.1063/1.4771722

Chelating heteroatomic conjugated molecules, such as pyridine, benzoxazole, and benzothiazole derivatives, are technologically important compounds. An increasing research focus for heteroatomic conjugate molecules is their application in the area of organic optoelectronic materials, such as photoconducting materials [8], liquid crystals [9], and fluorophores [10-12]. Heteroatomic conjugate molecules have also been widely used as cyclometalated ligands in heavy metal complexes because of their strong chelating capability and their characteristic optical properties based on π-conjugation. Heavy metal complexes, such as Ir(III) [13] and Pt(II) [14] complexes, have been proven to be excellent phosphorescent dyes for the organic light-emitting diodes.

Cinnamates also have received much attention, as they are the most widely used UVB blocking compounds among the various cosmetic sunscreen agents [15,16]. Cinnamates achieve UVB blocking from a ππ* absorption followed by a *cis–trans* isomerization at the propenyl double bond in the S_1 state and a relaxation to the ground state involving nonradiative decay [17,18]. As a UVB blocking compound, the optical properties, in particular the photoabsorption efficiency in the UVB energy region (290–320 nm) is an important factor. In order to achieve the favorable optical properties, molecular design using the variation of the substituents has been intensively performed [19].

The SAC [20]/SAC–CI (symmetry-adapted cluster-configuration interaction) method [21-23] has been shown to be reliable and useful for investigating a wide variety of chemistry and physics [24]. The method has been applied to the molecular spectroscopies including valence [25-27] and inner-shell excited states [28-30], molecular structure and spectroscopic constants in the excited states [31-34], catalytic reactions [35] and surface photochemistry [36], photochemical reactions [37], biological photochemistry and electron transfer [38-41], atmospheric chemistry [42,43], molecular interaction [44], and magnetic chemistry including ESR hyperfine splitting constants [45]. From these applications, the SAC-CI method has been established as a reliable methodology for investigating the electronic structure of molecules in ground, excited, ionized, and electron-attached states. The analytical energy gradient of the SAC-CI method is formulated and implemented [31,32]. The method was also extended to more complex electronic states[33,34] and the stable geometry optimization[46,47] is possible for the molecular excited states. The method was implemented in the Gaussian 03 suite of programs [48].

In this article, we review our recent SACI-CI studies on the electronic structure and optical properties of some conjugated molecules. We first introduce the SAC-CI theory briefly in particular SAC-CI SD-*R* method which is useful for investigating the large molecular system. We then explain the recent applications to the excited states of π-conjugated molecules like the OLED molecular systems [49,50], chelating heteroatomic conjugated ligands [51], and the UVB blocking molecules [52]. For OLED, we introduce the works of poly *para*-phenylene vinylene, poly *para*-phenylene, and fluorene-thiophene. For the chelating hetero-atomic conjugate molecules, photo-physical properties of 2-phenyl pyridine (PPY), 2-phenyl quinoline (PQ), and bonzo[h]quinoline (BZQ) that are widely used for developing iridium (III) complexes, are introduced. Theoretical work on the methoxy substituted cinnamates, which show excellent UVB blocking performance, is reviewed. The target molecules are ortho-, meta-, and para-monomethoxy substituted cinnamates, and 2,4,5- and 2,4,6-trimethoxy cinnamates in both *cis*- and *trans*- isomers. The difference in electronic transitions among these molecules and the effect of methoxy substitution at the ortho-, meta-, and para-positions are analyzed. The energy relaxation paths which lead to the non-radiative decay through the conical intersection are also addressed briefly.

SAC-CI METHOD

The SAC wave function describes the ground state and is defined as [20]

$$\Psi_g^{SAC} = \exp(\sum_I C_I S_I^\dagger)|0\rangle, \tag{1}$$

where $|0\rangle$ is the Hartree–Fock wave function and $S_I^\dagger$ is the spin-symmetry- and space-symmetry-adapted excitation operator. In the SAC method, to solve for C_I we require that the Schrödinger equation is satisfied within the configuration space of $\{|0\rangle, S_I^\dagger|0\rangle\}$ as

$$\langle 0|H - E_g|\Psi_g^{SAC}\rangle = 0, \tag{2}$$

$$\langle 0|S_I\left(H - E_g\right)|\Psi_g^{SAC}\rangle = 0. \tag{3}$$

This SAC equation is called a nonvariational method.

The SAC theory defines not only the SAC wave function for the ground state, but also the excited functions that span the basis for the excited states. Using the correlated ground-state SAC wave function, we define the excited functions $\{\Phi_K\}$ as

$$\Phi_K = PR_K^\dagger \left|\Psi_g^{SAC}\right\rangle, \tag{4}$$

where P is an operator that projects out the ground state and $\{R_K^\dagger\}$ represents a set of the excitation, ionization, and electron-attachment operators. These functions $\{\Phi_K\}$ constitute a basis for the excited state. Therefore, we describe the excited state by a linear combination of these functions as

$$\Psi_e^{SAC-CI} = \sum_K d_K \Phi_K , \tag{5}$$

which is the SAC–CI expansion. The non-variational SAC–CI solution is obtained by projecting the Schrödinger equation to the $\{R_K^\dagger|0\rangle\}$ configuration space [21-23],

$$\left\langle 0\left| R_K \left(H - E_e\right)\right|\Psi_e^{SAC-CI}\right\rangle = 0 . \tag{6}$$

The electron correlation of the ground state is well described by SAC and the SAC–CI wave function describes a modification of the electron correlation by excitation. Therefore, the convergence of the SAC–CI expansion is much faster than calculating the excited-state correlations from the beginning.

There are two standards in the SAC-CI method with respect to the *R*-operators. The SAC-CI SD-*R* method is to include single and double excitation operators within the *R*-operators, for example, the SD-*R* wave function for the singlet excited states is,

$$\Psi_{SD-R}^{SAC-CI} = \left(\sum_{ia} d_i^a R_i^a + \sum_{ijab} d_{ij}^{ab} R_{ij}^{ab}\right)\exp\left(\sum_I C_I S_I\right)|0\rangle . \tag{7}$$

This method is accurate and efficient for the one-electron processes. The method has been widely applied to the molecular spectroscopy, biological chemistry, and surface chemistry. The other choice is to include not only single and double excitation operators, but also triple- and quadruple- and higher-excitation operators for the *R*-operators. The method is called as SAC-CI general-*R* method [53-55] and is necessary for investigating the multi-electron processes in the excitation and ionization phenomena. For the works in the present article, the system sizes are large and the excitations are described by the one-electron processes, and therefore, we used the SD-*R* method.

RESULTS AND DISCUSSION

Organic Light-Emitting Diodes

Organic light-emitting diodes are one of the promising candidates for the next generation electro-optical devices such as panel display. Theoretical prediction of the photo-physical properties of the OLED is relevant for the molecular design. The excited-state chemistry of the OLED contains the interesting issue like localization/delocalization of the excitation and the effect of the flexible conformation. We have studied the absorption and emission spectra and the excited-state geometries of some OLED molecules such as poly *para*-phenylene vinylene (PPV) and poly *para*-phenylene (PP) [49], fluorene-thiophene (FT) and its derivatives [50]. In the present article, we introduce the excited states of PPV and FT.

The optical properties of poly *para*-phenylenevinylene (PPV) that is well-known as an efficient light emitter have been extensively investigated [1-4], however, the accurate theoretical prediction of the transition energies is still challenging. The electronic spectra and excited-state geometry of the PPV oligomer (Fig. 1) were investigated by the SAC-CI SD-*R* method. The calculated absorption and emission energies of the lowest singlet (S_1) excited state of PPVn (n=1~4) are compared with the experimental values [4] and other theoretical values [56,57] in Fig. 2. The SAC-CI method predicted the experimental values in high accuracy; the mean deviations are 0.09 eV for absorption and 0.03 eV for emission. The method reproduced the chain-length dependence of the excitation energy better than the TDDFT/B3LYP calculations. The conventional TDDFT should be carefully used for the transition energies of the molecules with long π-conjugated chains.

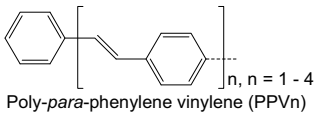

FIGURE 1. Molecular structure of PPVn oligomer.

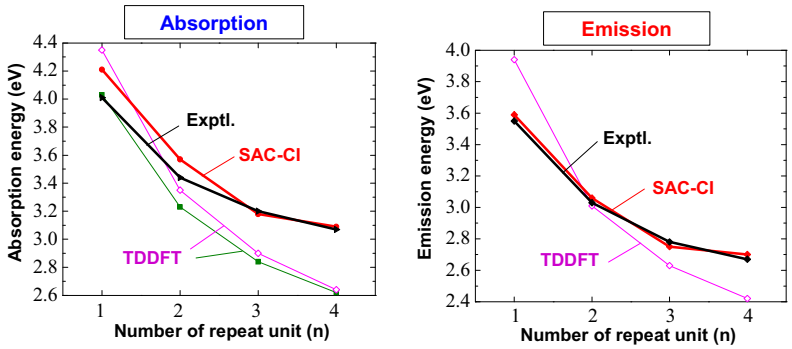

FIGURE 2. Excitation (left) and emission (right) energies of PPVn (n=1-4) plotted to the repeat unit n.

The ground-state and lowest singlet and triplet excited-state structures of PPVn were calculated to be planar by the SAC-CI method. The calculated ground-state geometry agrees very well with the experimental values; the deviations are within 0.005 Å and 0.07˚ for the bond length and bond angle, respectively, for PPV1. The changes in bond length (Δr) along the CC conjugation due to singlet and triplet excitations of PPV1 are shown in Fig. 3. In the S_1 and T_1 states, the central vinylene C=C bond length increases, whereas the vinylene C-C bond length decreases. These changes are localized in the central part of the PPVn oligomers. The bond length alternation changes significantly in the excited states from that of the ground state. Larger bond length changes were obtained for the T_1 state than for the S_1 state.

These changes in the geometry due to excitation can be explained using the ESF theory [58,59]. In ESF theory, the geometric relaxation in the excited state can be explained by the force acting on nuclei caused by changes in the electron distribution. Molecular shape in the ground and excited states is determined by the balance of the atomic dipole (AD), exchange (EC), and gross charge (GC) forces. The SAC/SAC-CI electron density difference between the ground and S_1 states due to excitation of PPV1 is shown in Fig. 4. The electron density in the central vinylene C=C bond region decreases, and that in the vinylene C-C bond region increases. More precisely, the electron density in the σ-bond region increases, and that in the π-bond region decreases; this is a general trend in these PPVn molecules. The EC force along the central vinylene C=C bond decreases because of the decrement of electron density in the C=C bond region, whereas the EC force is enhanced along the vinylene C-C bond. Consequently, the central vinylene C=C bond length increases, and the vinylene C-C bond length decreases. The accumulations (depletions) of electron density in the vicinity of C nuclei also explain the bond angle change in the excited states. For example, in PPV1, angle A3 (Fig. 17) is enlarged in the singlet excited state (119.4˚) from that in the ground state (118.3˚) as a result of an accumulation of electron density in the region of the associated C nucleus.

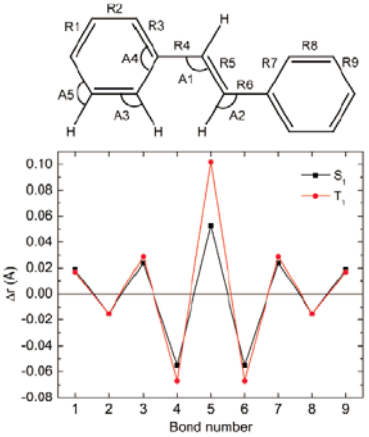

FIGURE 3. CC bond length change in the S_1 and T_1 states of PPV1.

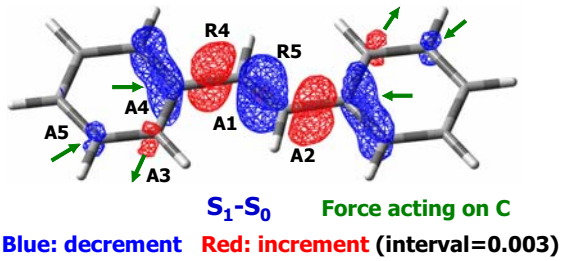

FIGURE 4. Electron density difference between the S_0 and S_1 states calculated by the SAC/SAC-CI method.

Conformational effect of fluorene-thiophene and its derivative on electronic spectra

The fluorene co-polymers constitute rigorous candidates for the flexible and tunable light-emitting diodes [5-7]. By introducing the suitable substituents, the optical properties can be controlled because of its flexible structure. In particular, fluoerene-thiphene co-polymers have been focused since they are the candidates for the blue-light emitter. The unit of these co-polymers, fluorene-thiophene (FT) and fluorene-methyl-thiophene (FMT) (Fig. 5) show the characteristic electronic spectra [60-62]. The energy region of the absorption spectrum is almost the same, however, the shape of the electronic spectra of these molecules are different. To interpret the difference of the spectra, the ground and excited states of these molecules and the conformational effect on the electronic spectra were investigated by the SAC-CI method [50].

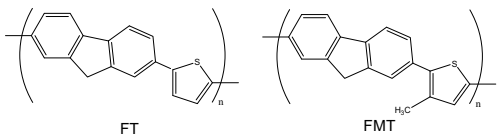

FIGURE 5. Molecular structures of FT and FMT oligomers.

The ground-state potential energy curves of the FT and FMT monomers along the torsion angle are shown in Fig. 6. The dihedral angles of the most stable conformation of FT and FMT are θ=27° and 43°, respectively. These molecules have very flexible structure with regard to the torsion. The potential energy curves are very flat for the torsion; the relative energy of the conformers for θ=0°~60° are within about 1.0 kcal/mol. This low rotational energy barrier indicates that it allows a wide range of nonplanar conformation of these molecules at room temperature.

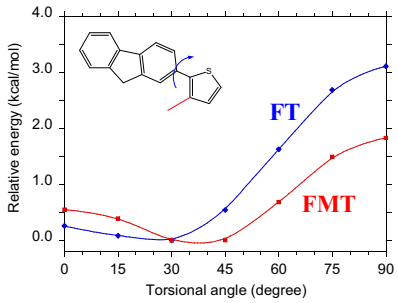

FIGURE 6. The ground-state potential energy curves of FT and FMT monomers.

The optical properties of the low-lying excited states of these molecules are dependent on the torsion angle. The excitation energy and oscillator strength as the function of the torsion angle are displayed in Fig. 7. The first to third excited states interact to each other along the torsion. The avoided crossing occurs between the first and third excited states in the region of θ=30°~60°; this interaction is clearly seen in the oscillator strength.

Since the ground-state potential energy surfaces are flat for the torsion and the excitation spectra are dependent on this coordinate, thermal average of the conformers should be considered in order to simulate the absorption spectra. The simulated absorption spectra of FT and FMT, in which thermal distribution at 298 K is taken into account, are compared with the experimental spectra in Fig. 8. The simulated spectra with thermal average showed excellent agreement with the experimental spectra. For FT, the contribution of the conformer whose torsion angle is up to θ=~30° is dominant and the asymmetric spectrum is obtained. In the case of FMT, the strong shoulder was measured in the higher energy side of the peak. This shoulder is attributed to the second excited state of the conformer of θ=30°~45°.

The SAC-CI calculations show that the thermal average of the conformers is important to interpret the electronic spectra of the fluorene-thiophene co-polymer.

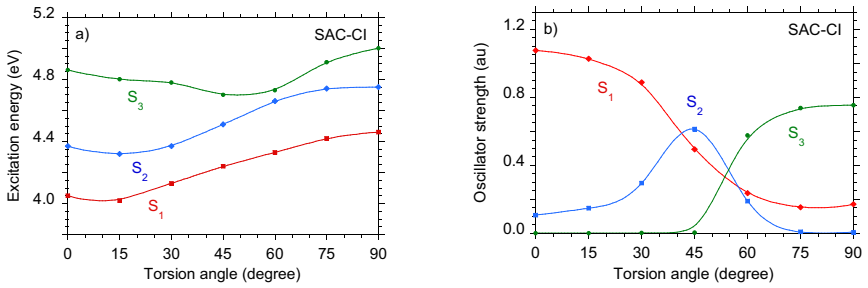

FIGURE 7. SAC-CI (a) excitation energy and (b) oscillator strength of the first three excited states of FT versus torsion angle.

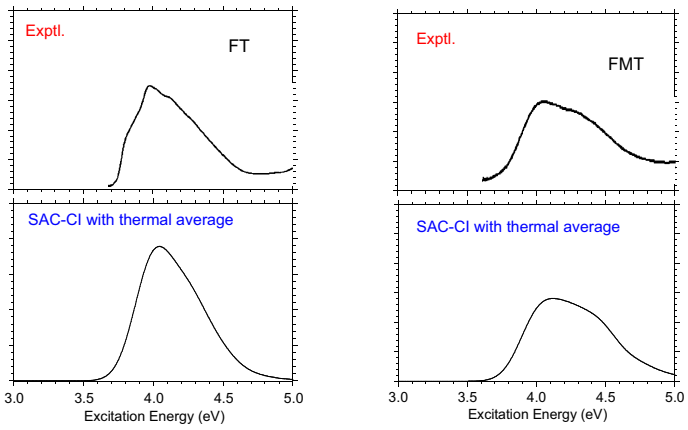

FIGURE 8. Experimental and SAC-CI absorption spectra of FT and FMT.

Chelating Hetero-Atomic Conjugated Molecules

We studied the electronic structure and optical properties of the 13 chelating hetero-atomic conjugated molecules, including 2-phenyl pyridine (PPY), 2-phenyl quinoline (PQ), bonzo[h]quinoline (BZQ), 2,5-diphenyl-oxazole (DPO), 2-phenyl-benzoxazole (BO), 1-(1-naphthyl)-benzoxazole (BON), 2-phenyl-oxazoline (OP), 2-phenyl-benzothiazole (BT), 2-(2-benzothienyl)-pyridine (BTP), 2-(1-naphthyl)-benzothiazole (αBSN), 2-(2-naphthyl)-benzothiazole (βBSN), 2-(2-thienyl)-pyridine (THP), and 2-(2-thienyl)-benzothiazole (BTTH), by the SAC–CI method [51]. These molecules can be categolized into three group: I) PPY, PQ, and BZQ; II) DPO, BO, BON, and OP; and III) BT BTP, αBSN, βBSN THP, and BTTH, based on the heteroatoms in their molecular structures. In this article, we introduce the results of the molecules in group I.

Each compound in this group I contains one N atom in the conjugated ring. Figure 9 illustrates the calculated geometries of PPY, PQ and BZQ in the ground state (S_0) and the lowest $\pi\pi^*$ excited state (S_1) with the CC bond lengths. In the S_0 state of PPY, a non-planar structure is most stable with the torsion angle of 20.4°; the energy difference between planar and non-planar structure is about 0.2 kcal/mol. The PQ also has non-planar geometry at the S_0 state with =21.0°. These molecules becomes planar from a non-planar structure by the S_0-S_1 excitation. For PPY, the inter-ring CC bond distance is 1.488Å in S_0 and the bond shrinks significantly to 1.407Å in S_1. The bonds in the pyridyl and phenyl rings also become elongated or shorten alternatively by the S_0–S_1 excitation. The same trend was also found in PQ: it becomes planar in S_1 and the inter-ring CC bond becomes significantly shortened from 1.491Å in S_0 to 1.427Å in S_1, and the other bonds in the rings change alternatively. Finally, when BZQ is excited to an S_1 state, bonds in this fused ring molecule become shortened or elongated, but there is no dominant bond-distance change in a single pair of atoms, as the geometry relaxation spreads out almost evenly over the entire molecule.

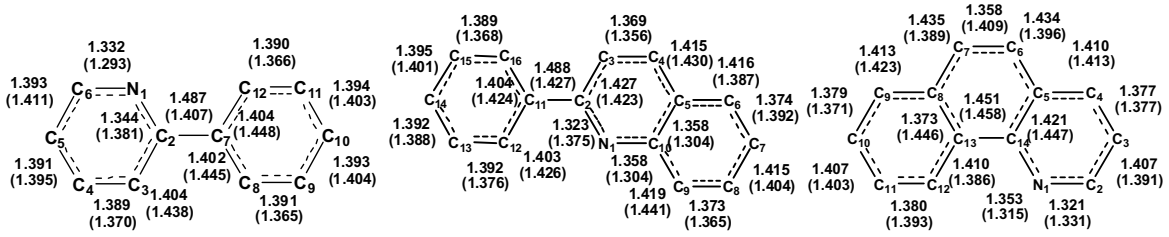

(a) PPY (b) PQ (c) BZQ

FIGURE 9. Geometries of PPY, PQ, and BZQ in the S_0 and S_1 states. Values are bond lengths of the S_0 (S_1) states.

The geometry relaxation in the excited state can be interpreted using the ESF theory [58,59] as discussed in the case of PPVn. As an example, we discuss the geometric changes in the S_1 state of PPY. In ESF theory, geometry relaxation in the excited state is due to the force acting on nuclei caused by changes in electron distribution. The differences in the SAC–CI electron density between the S_0 and S_1 states in PPY and BZQ are shown in Fig. 10. In PPY, the electron density in the C–C (C_2–C_3, C_7–C_{12}, C_7–C_8) and C_2=N_1 bonds in the phenyl ring and pyridyl ring decrease, while the density of the inter-ring C_2–C_7 bond significantly increases. The EC force along bonds including the C_2=N_1 and C_2–C_3 bonds decreases because of the decrement of electron density, whereas the EC force is enhanced along the C_2–C_7, C_6–N_1, and C_3–C_4 bonds. Consequently, the former bond lengths increase, and the latter bond lengths decrease. This geometry change enhance the conjugation between two rings and the S_1 structure of PPY becomes planar.

(a) PPY (b) BZQ

FIGURE 10. The SAC–CI electron density difference between the S_0 and S_1 states of PPY and BZQ. The region in the blue range has a decrement of electron density and that in the red range has an increment of electron density when a molecule is excited.

The experimental and theoretical absorption spectra of PPY and PQ are compared in Fig. 11. The calculated spectra satisfactorily reproduced the position of the observed absorption peaks for these molecules. Based on the SAC–CI calculations, we assign the broad peak around 4.49eV (276 nm) as the second and third transitions calculated as 4.49eV and 4.69eV. The peak around 5.14eV (242nm) is assigned as the transition with a vertical excitation energy of 5.15eV. These transitions are mainly due to ππ* transitions. The SAC–CI calculation for PQ shows that the strongest transition occurs at an energy of 5.22eV. The experimental spectrum gives a strong indication that the absorption is very strong above 4.76eV (260nm). The absorption energies of 3.87eV and 4.49eV in our calculations are consistent with the structures at 3.87eV (320nm) and 4.35eV (285nm) in the experimental absorption spectra.

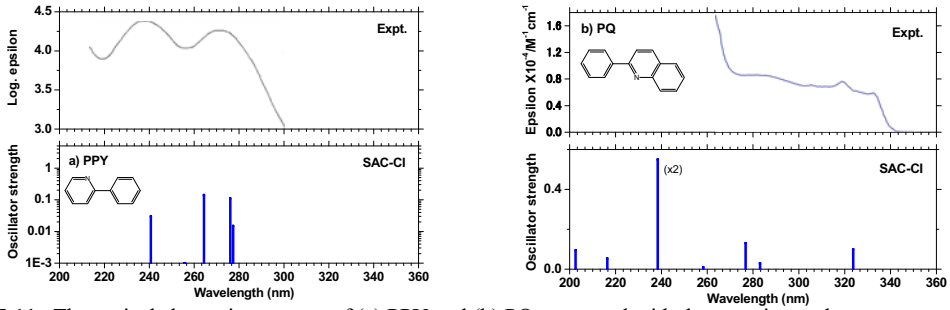

FIGURE 11. Theoretical absorption spectra of (a) PPY and (b) PQ compared with the experimental spectra.

UVB Blocking Cinnamates

The electronic structure and optical properties of the *cis*- and *trans*-isomers of methoxy substituted cinnamates have been investigated using the SAC-CI method. The molecules are ortho-(**1**), meta-(**2**), and para-(**3**) monomethoxy substituted cinnamates, and 2,4,5-(**4**) and 2,4,6-(**5**) trimethoxy cinnamates as shown in Fig. 12. In this article, we focus on the results of the *trans* isomers of the compounds **1**, **2**, and **3**. The trend of *cis*-isomers is similar to that of *trans*-isomers and the results of tri methoxy derivatives can be referred to ref. [52].

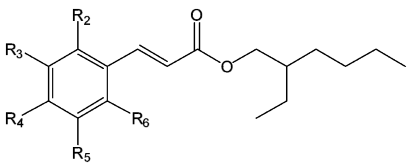

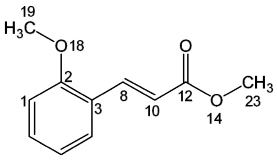

Mol.	R_2	R_3	R_4	R_5	R_6
1	OCH_3	H	H	H	H
2	H	OCH_3	H	H	H
3	H	H	OCH_3	H	H
4	OCH_3	H	OCH_3	OCH_3	H
5	OCH_3	H	OCH_3	H	OCH_3

FIGURE 12. Chemical structures of 2-ethylhexyl-cinnamate derivatives and the calculated model compounds of trans-isomers.

The S_0 and S_1 state geometries of the *trans*-isomers of ortho-(**1**), meta-(**2**), and para-(**3**) methoxy substituted compounds were shown in Fig. 13. All the compounds, except for the *cis*-**5** compound, had local minima in the coplanar structure of the *cis*- and *trans*-isomers in both the S_0 and S_1 states due to π-conjugation. In the S_0 state, the rotational energy barrier of the methoxy group is very low, although the planar structure is the most stable structure. The global minimum of the S_1 state is in the form of a nonplanar structure, but local minimum exist in the planar structure. The emission was observed from this local minimum in the planar structure, and in particular, a strong emission was observed for compound **2**.[5]

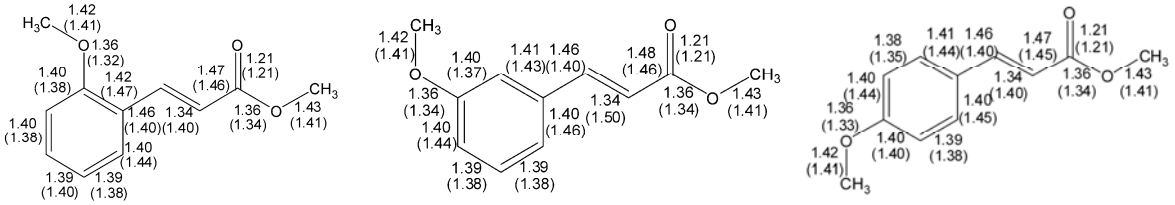

FIGURE 13. CC and CO bond length of the S_0 and S_1 states (in parentheses) of *trans*-**1**, *trans*-**2**, and *trans*-**3**.

It was found that the C_1–C_2, C_3–C_8, C_{10}–C_{12}, C_{12}–O_{14}, and O_{14}–C_{23} bond lengths decrease and the length of the other bonds increases. In the S_0 state, the carbon–carbon bond alternation exists for both the single and double bonds, but this bond alternation relaxes in the S_1 state. Since the excitation is relatively localized in the central unit, the prominent changes occur in the vinylene unit. For example, in the *trans*-**1** compound, the change in bond length is Δr = +0.048, –0.060, and +0.057 Å for C_2–C_3, C_3–C_8, and C_8–C_{10}, respectively, while the other changes in bond length are within 0.022 Å.

The absorption spectra of the methoxy substituted cinnamates were calculated. The SAC-CI excitation spectra for the monomethoxy substituted molecules are compared with the experimental absorption spectra in Fig. 14. For the monomethoxy substituted compounds, the excited states that contribute to the absorption have a different character that depends on the methoxy substituted position. In the case of the ortho-(*trans*-**1**) and meta-(*trans*-**2**) compounds, the S_3 state has the highest transition probability, and is characterized as being the transition from the next HOMO to LUMO (nH–L) transition, whereas, the highest transition possibility of the para-(*trans*-**3**) compound was calculated for the $S_0 \rightarrow S_1$ transition, and the excitation character is a HOMO–LUMO (H–L) transition. The agreement with the experimental values was satisfactory; the deviations were within about 10 nm.

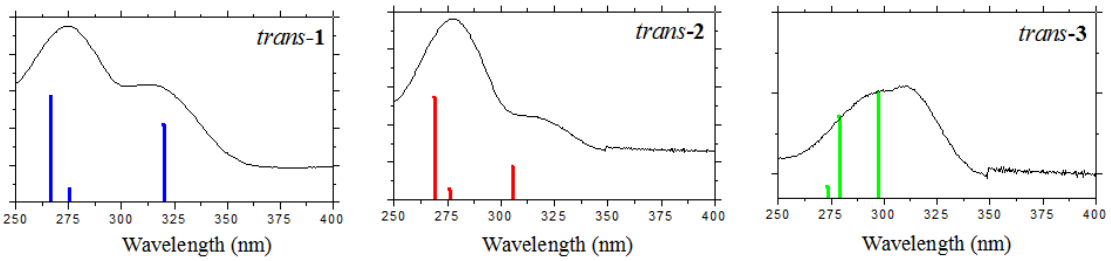

FIGURE 14. SAC-CI absorption spectra of trans-**1**, **2** and **3** compounds compared with the experimental spectra [19].

The emission energies of these molecules have also been calculated using the SAC-CI method. The stable geometries of the S_1 state were located using CIS followed by the SAC-CI calculations of the vertical emission energies. The calculated emission energies are in good agreement with the experimental data as shown in Table 1. In general, the SAC-CI calculations reproduced the experimental trends observed in hexane solution satisfactorily. The emission energies of molecules were in the order of: compounds **2** and **3** (~350 nm) < compounds **1** (~360 nm). The deviation from the experimental values was within 10 nm. The transition was characterized as the HOMO–LUMO transition, and the SAC-CI coefficients are localized for this configuration. The calculated oscillator strengths were in the range 0.41–0.68 for all the molecules. As shown in the absorption data, the S_1 state of compound **2** also had a low oscillator strength in the ground state geometry, and the transition probability is distributed to the S_3 state. The calculated Stokes shifts were 0.40–0.50 eV for compounds **1** and **2** and these were slightly larger, 0.58 eV for compounds **3** where the para-position is substituted by a methoxy group. This means that the excited state geometry relaxations in the S_1 state of compounds **3** are larger than those for compounds **1** and **2**.

TABLE 1. Emission energy (ΔE), emission wavelength (λ_{max}), oscillator strength (f) calculated using the SAC-CI method. Experimental values are cited from Ref. 5.

Mol.	**SAC-CI**			**Expt.**
	ΔE (eV)	λ_{max} (nm)	f	λ_{max} (nm) in hexane
trans-**1**	3.37	367	0.44	359
trans-**2**	3.62	343	0.29	350
trans-**3**	3.52	352	0.61	351

The energy relaxation processes in the excited states are important for the UVB blocking molecules. We examined the S_1 potential energy surface of *trans*-**2** and *trans*-**3** which mainly leads to decay by fluorescence and non-radiative decay through conical intersection, respectively. Since the SAC-CI method is based on the single-reference theory, it is difficult to obtain the potential energy surface around the conical intersection. We performed the SAC-CI partial optimization of the S_1 state for the torsion angles from 0 to 75 degrees with all the other coordinates being optimized. The small basis sets and restricted active space were used and the perturbation selection of the operator was not performed in the SAC-CI calculations. In *trans*-**2**, the energy barrier to the conical intersection was calculated to be about 5.5 kcal/mol (0.24 eV), while *trans*-**3** has almost no energy barrier. These calculations qualitatively explain the experimental fact that the activation energies based on the non-radiative deactive rate.

SUMMARY

The SAC-CI theoretical spectroscopy has been applied to the electronic structure and optical properties of some organic conjugated molecules, that is the oligomers for organic-light emitting diodes (OLED), chelating hetero-atomic conjugated ligands, and UVB blocking molecules.

The absorption and emission spectra of these molecules were reproduced accurately. For OLED molecules, chain length dependence of the excitation and emission energies was well reproduced for poly *para*-phenylene vinylene and poly *para*-phenylene. Thermal effect on the electronic spectrum of fluorene-thiophene and its derivatives as well as its oligomers was found to be important to interpret the electronic spectra. The photo-physical properties of the chelating hetero-atomic molecules including pyridine-, benxazole-, and benzothiazole derivatives was systematically calculated and predicted. The UVB blocking function of the methoxy substituted cinnamates was investigated with regard to the substitution position. The energy relaxation processes in the excited states of cinnamates was also addressed. The excited-state geometry relaxation of these molecules was interpreted based on the electrostatic force theory.

The present work provides a useful basis for the theoretical design predicting the optical properties of the photo-functional molecules.

ACKNOWLEDGMENTS

This study was supported by the grant from the JST-CREST, Scientific Research in Priority Areas “Molecular Theory for Real Systems” from the Ministry of Education, Culture, Sports, Science and Technology of Japan, the Next Generation Supercomputing Project, and the Molecular-Based New Computational Science Program, NINS. The part of the computations were performed using Research Center for Computational Science, Okazaki, Japan.

REFERENCES

1. J. H. Burroughes, D. D. C. Bradley, A. R. Brown, R. N. Kckay, R. H. Friend, P. L. Burn, and A. B. Holmes, *Nature* **347**, 539 (1990).
2. N. Tessler, G. J. Denton, and R. H. Friend, *Nature (London)* **382**, 695 (1996).
3. R. H. Friend, R. W. Gymer, A. B. Homes, J. H. Burroughes, R. N. Marks, C. Taliani, D. D. C. Bradley, D. A. D. Santos, J. L. Bredas, M. Loglund, and W. R. Salaneck, *Nature (London)* **397**, 121 (1999).
4. J. Gierschner, H.-G. Mack, L. Luer, and D. Oelkrug, *J. Chem. Phys.* **116**, 8596 (2002).
5. L. Feng, E. Zhang, H. Bie, and Z. Chen, *Dyes Pigments* **64**, 31 (2005).
6. F. I. Wu, C. F. Shu, C. H. Chien, and Y. T. Tao, *Syn. Met.* **148**, 133 (2005).
7. D. H. Hwang, M. J. Park, and J. H. Lee, *Mater. Sci. Eng. C* **24**, 201 (2004).
8. C. Kalle, *Patent No. 895001* (1962).
9. A. Mori, A. Sekiguchi, K. Masui, T. Shimada, M. Horie, K. Osakada, M. Kawamoto, and T. Ikeda, *J. Am. Chem. Soc.* **102**, 1700 (2003).
10. D. L. Williams and A. Heller, *J. Phys. Chem.* **74**, 4473 (1970).
11. P. F. Barbara, L. E. Brus, and P. M. Rentzepis, *J. Am. Chem. Soc.* **102**, 5631 (1980).
12. R. S. Becker, C. Lenolele, and A. Zein, *J. Phys. Chem.* **91**, 3509 (1987).
13. S. Lamansky, P. Djurovich, D. Murphy, F. Abdel-Razzaq, H. F. Lee, C. Adachi, P. E. Burrows, S. R. Forrest, and M. E. Thompson, *J. Am. Chem. Soc.* **123**, 4304 (2001.).
14. J. Brooks, Y. Babayan, S. Lamansky, P. I. Djurovich, I. Tsyba, R. Bau, and M. E. Thompson, *Inorg. Chem.* **41**, 3055 (2002).
15. T. Monhapol, B. Albinsson, and S. Pattanaargson, *J. Pharm. Pharmacol.* **59**, 279 (2007).
16. L. Oriol, M. Pinol, J. L. Serrano, and R. M. Tejedor, *J. Photochem. Photobiol. A.* **155**, 37 (2003).
17. S. Pattanaargson and P. Limphong, *Int. J. Cosmet. Sci.* **23**, 153 (2001).
18. H. B. Wang, B. C. Zhai, W. J. Tang, J. Y. Yu, and Q. H. Song, *Chem. Phys.* **333**, 229 (2007).
19. T. M. Karpkird, S. Pattanaargson, and B. Albinsson, *Photochem. Photobiol. Sci.* (in press).
20. H. Nakatsuji and K. Hirao, *J. Chem. Phys.* **68**, 2053 (1978).
21. H. Nakatsuji, *Chem. Phys. Lett.* **59**, 362 (1978).
22. H. Nakatsuji, *Chem. Phys. Lett.* **67**, 329 (1979).
23. H. Nakatsuji, *SAC-CI method: Theoretical aspects and some recent topics, in Computational Chemistry, Review of Current Trends*. (World Scientific, Singapore, 1997).
24. M. Ehara, J. Hasegawa, and H. Nakatsuji, *SAC-CI Method Applied to Molecular Spectroscopy, in Theory and Applications of Computational Chemistry: The First 40 Years,*. (Elsevier, Oxford, 2005).
25. J. Wan, M. Ehara, M. Hada, and H. Nakatsuji, *J. Chem. Phys.* **113**, 5245 (2000).
26. J. Wan, M. Hada, M. Ehara, and H. Nakatsuji, *J. Chem. Phys.* **114**, 5117 (2001).
27. B. Saha, M. Ehara, and H. Nakatsuji, *J. Chem. Phys.* **125**, 014316 (2006).
28. M. Ehara, H. Nakatsuji, M. Matsumoto, T. Hatamoto, X.-J. Liu, T. Lischke, G. Prümper, T. Tanaka, C. Makochekanwa, M. Hoshino, H. Tanaka, J. R. Harries, Y. Tamenori, and K. Ueda, *J. Chem. Phys.* **124**, 124311 (2006).
29. M. Ehara, K. Kuramoto, H. Nakatsuji, M. Hoshino, T. Tanaka, M. Kitajima, H. Tanaka, Y. Tamenori, A. D. Fanis, and K. Ueda, *J. Chem. Phys.* **125**, 114304 (2006).
30. M. Ehara and H. Nakatsuji, *Coll. Czech. Chem. Commun* **73**, 771 (2008).
31. T. Nakajima and H. Nakatsuji, *Chem. Phys. Lett.* **280**, 79 (1997).
32. T. Nakajima and H. Nakatsuji, *Chem. Phys.* **242**, 177 (1999).
33. M. Ishida, K. Toyoda, M. Ehara, and H. Nakatsuji, *Chem. Phys. Lett.* **350**, 351 (2001).
34. M. Ishida, K. Toyoda, M. Ehara, M. J. Frisch, and H. Nakatsuji, *J. Chem. Phys.* **120**, 2593 (2004).
35. H. Nakatsuji and H. Nakai, *J. Chem. Phys.* **98**, 2423 (1993).
36. H. Nakatsuji, R. Kuwano, H. Morita, and H. Nakai, *J. Mol. Catalysis* **82**, 211 (1993).
37. M. Hada, Y. Imai, M. Hidaka, and H. Nakatsuji, *J. Chem. Phys.* **103**, 6993 (1995).
38. H. Nakatsuji, J. Hasegawa, and K. Ohkawa, *Chem. Phys. Lett.* **296**, 499 (1998).
39. J. Hasegawa and H. Nakatsuji, *J. Phys. Chem. B* **102**, 10420 (1998).
40. K. Fujimoto, J. Hasegawa, S. Hayashi, S. Kato, and H. Nakatsuji, *Chem. Phys. Lett.* **414**, 239 (2005).
41. N. Nakatani, J. Hasegawa, and H. Nakatsuji, *J. Am. Chem. Soc.* **129**, 8756 (2007).
42. S. Arulmozhiraja, R. Fukuda, M. Ehara, and H. Nakatsuji, *J. Chem. Phys.* **124**, 034312 (2006).
43. M. Ehara, Y. Ohtsuka, and H. Nakatsuji, *Chem. Phys.* **226**, 113 (1998).

44. M. Ehara and H. Nakatsuji, *J. Chem. Phys.* **102**, 6822 (1995).
45. H. Nakatsuji, M. Ehara, and T. Momose, *J. Chem. Phys.* **100**, 5821 (1994).
46. K. Toyota, M. Ehara, and H. Nakatsuji, *Chem. Phys. Lett.* **356**, 1 (2002).
47. K. Toyota, M. Ishida, M. Ehara, M. J. Frisch, and H. Nakatsuji, *Chem. Phys. Lett.* **367**, 730 (2003).
48. M. J. Frisch et al., *GAUSSIAN 03* (Gaussian Inc., Pittsburgh, PA, 2003).
49. B. Saha, M. Ehara, and H. Nakatsuji, *J. Phys. Chem. A* **111**, 5473 (2007).
50. P. Poolmee, M. Ehara, S. Hannongbua, and H. Nakatsuji, *Polymer* **46**, 6474 (2005).
51. Y. Lu and M. Ehara, *Theor. Chem. Acc.* (in press).
52. M. Promkatkaew, S. Suramitr, T. M. Karpkird, S. Namuangruk, M. Ehara, and S. Hannongbua, (submitted).
53. H. Nakatsuji, *Chem. Phys. Lett.* **177**, 331 (1991).
54. M. Ehara and H. Nakatsuji, *Chem. Phys. Lett.* **282**, 247 (1998).
55. M. Ehara, M. Ishida, K. Toyota, and H. Nakatsuji, *SAC-CI general-R method: Theory and Applications to the Multi-Electron Processes, in Reviews in Modern Chemistry*. (World Scientific, Singapore, 2002).
56. A. Pogantsch, G. Heimel, and E. Zojer, *J. Chem. Phys.* **117**, 5921 (2002).
57. Y. Han and S. U. Lee, *J. Chem. Phys.* **121**, 609 (2004).
58. H. Nakatsuji, *J. Am. Chem. Soc.* **95**, 345 (1973).
59. H. Nakatsuji and T. Koga, *The Force Concept in Chemistry*. (Van Nostrand Reinhold, New York, 1981).
60. M. Belletete, S. Beaupre, J. Bouchard, P. Blandin, M. Leclerc, and G. Durocher, *J. Phys. Chem. B* **104**, 9118 (2000).
61. M. Belletete, M. Dedard, M. Leclerc, and G. J. Durocher, *J. Mol. Structu. (THEOCHEM)* **679**, 9 (2004).
62. T. Tirapattur, M. Belletete, M. Leclerc, and G. J. Durocher, *J. Mol. Struct. (THEOCHEM)* **625**, 141 (2003).